



Optimized Bioleaching Pre-treatment of UG-2 PGM Flotation Concentrate Using Design of Experiments

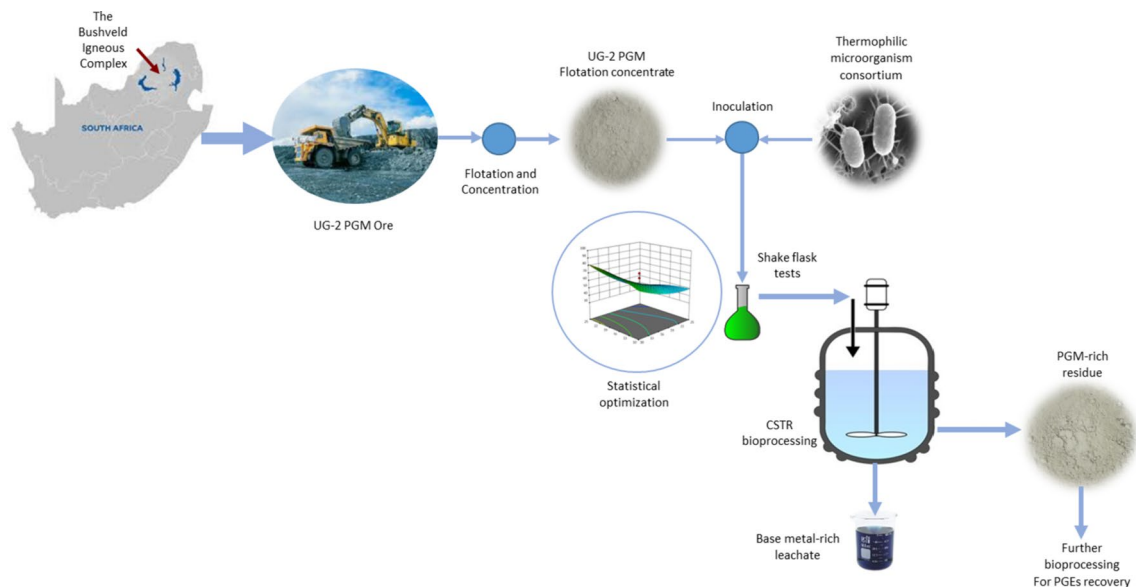
A. Shemi^{1,2} · L. Chipise^{1,2} · C. S. Yah^{2,4} · A. Kumar^{1,2} · S. Moodley^{1,2,3} · K. Rumbold³ · G. Simate¹ · S. Ndlovu^{1,2} 

Received: 25 June 2023 / Accepted: 23 January 2024
© The Author(s) 2024

Abstract

The depletion of the Merensky ore has led the South African platinum industry into largely mining and processing Upper Group Two (UG-2) ore for the extraction of Platinum Group Metals (PGMs). However, the processing of the UG-2 material is not fully amenable to the conventional pyrometallurgical route due to the high chrome content. Therefore, in this study, a bio-based process for base metal extraction from UG-2 flotation concentrates was investigated. This study represents only part of the work done in a broader investigation to develop a completely biological two-stage process for the extraction of base metals and PGEs. In this paper, only the first stage of the process is presented. This study evaluated a mixture of indigenous thermoacidophile archaeobacteria namely, *Acidianus brierleyi*, *Sulfolobus sp.*, and *Metallosphaera sedula*. A statistical Design of Experiments (DOE) was used for finding optimal conditions. Factors investigated included particle size, pH, pulp density, inoculum dosage, and temperature. Optimal extraction efficiencies of 92% for Co, 97% for Cu, and 99% for Ni were predicted at correlation coefficients of 92.5%, 93.2%, and 88.0%, respectively, thus, verifying the fitness of the model. Optimal base metal extractions obtained were 99.3% for Co, 90.1% for Cu, 41.58% for Fe, and 99.5% for Ni. The results showed a substantial extraction of base metals from UG-2 PGM flotation concentrate suggesting a potentially feasible option for industrial bioprocessing of PGM concentrates. To the best of the authors' knowledge, this is the first report on bioleaching of base metals from UG-2 flotation concentrates.

Graphical Abstract



The contributing editor for this article was Nikhil Dhawan.

Extended author information available on the last page of the article

Keywords PGMs · Base metals · Bioleaching · Thermophilic bacteria · Optimization

Introduction

Owing to their remarkable properties, platinum group metals (PGMs) are widely used in many industrial fields, most notably, as automobile exhaust catalysts [1]. The majority of the world's PGMs reserves (88%) are found in South Africa. The PGMs in South Africa are located in the Bushveld Igneous Complex which includes three distinct mineral-bearing reefs: the Merensky Reef, UG-2 Reef, and the Platreef [2–8]. The PGMs in the Merensky ore occur largely as sulfide minerals and partially as arsenides, tellurides, and ferroalloys [9–11]. The PGMs deport to the base metal sulfides [12]. Typically, the Merensky Reef has high quantities of sulfidic minerals, lower chromite values and contains relatively higher PGM grades, about 7–9 g/t [13–15]. The PGMs in the Platreef ore occur largely as Pd and Pt bismuth tellurides and arsenides which are observed to be slow floating in comparison to the PGM sulfides [16, 17]. The Platreef has high quantities of sulfidic minerals, similar to Merensky, but low PGM grade, about 1–4 g/t [15, 18] and relatively higher base metal content [2–8]. Thus, the reef is essentially a base metals and palladium resource rather than a traditional platinum resource [19]. The UG-2 reef is predominantly composed of chromite (60–90 wt%) as the abundant mineral, and the chromium oxide (chrome) content is averaged at 43.5 wt%. The base metal sulfide (BMS) minerals in UG-2 are present in trace amounts [11, 17]. The differences in mineralogy for the Merensky, UG-2, and Platreef ores are evident in Table 1 [20].

The advent of large-scale platinum production, in SA since 1928, was primarily based on the exploitation of the Merensky reef as it was classified as the most important source of PGMs in the world [13, 14, 21]). However, the South African (SA) platinum industry has advanced into an era of largely mining and processing the Upper Group Two (UG-2) ore of the Bushveld Igneous Complex (BIC). This course of direction has been caused by the depletion of easily available Merensky reserves and the scarcity of Platreef ore [22]. The mineralization of the UG-2 ore is unique and distinguishes it from its counterparts, the Merensky and Platreef ore bodies, which all lie in the BIC. The UG-2 Reef, typically, contains lower quantities of sulfide minerals, has high chromite content, and has a relatively lower PGM grade, about 6–8 g/t [15, 18, 23]. The mineralogy of the Merensky and Platreef flotation concentrates is similar, and both are amenable to conventional PGM smelting [6, 7]. In contrast, UG-2 concentrates are characterized by higher chromite content, typically > 3 wt%. The inherent high chrome grades have fundamentally rendered UG-2 concentrates unattractive and difficult to process using the current PGM smelting methods [22]. The high chrome content causes the chrome solubility limit in the silica glass phase to exceed the set limit of approximately <1.8 wt% [24], hence, leading to the formation of refractory chrome spinel phases and furnace run-outs [24–27], which in turn cause high energy consumption, poor smelting efficiency, and high operating costs. Various interventions ranging from the redesign and modification of existing physical and

Table 1 Typical bulk modal analysis of Merensky, UG-2, and Platreef ores [20]

Mineral name	Merensky Reef Volume %	UG-2 Reef	Platreef
Pyroxene (XYSi_2O_6)	55–60	15–30	30–40
Feldspar ($\text{CaAl}_2\text{Si}_2\text{O}_8$)	30–40	3–9	18
Chromite (FeCr_2O_4)	6	50–75	–
Talc ($\text{Mg}_3\text{Si}_4\text{O}_{10}(\text{OH})_2$)	< 1	< 1	< 1
Serpentine ($\text{Mg}_3\text{Si}_2\text{O}_5(\text{OH})_4$)	2–3	1	5
Amphibole ($(\text{Ca}, \text{Na})_2(\text{Mg}, \text{Fe}, \text{Al})_5(\text{Al}, \text{Si})_8\text{O}_{22}(\text{OH})_2$)	1–2	< 1	4
Chlorite ($(\text{Mg}, \text{Fe})_5\text{Al}(\text{Si}_3\text{Al})\text{O}_{10}(\text{OH})_8$)	1–2	< 1	4
Mica ($\text{K}(\text{Mg}, \text{Fe})_3\text{AlSi}_3\text{O}_{10}(\text{F}, \text{OH})_2$)	< 1	< 1	1
BMS	< 1	< 1	2
Other*	1–2	< 1	5

*Other minerals are mainly other silicates, Fe-oxides, and carbonates

X and Y are either both divalent cations (mainly Ca, Fe, Mg), or mono- (Na, Li) and trivalent cations (Al, Fe), respectively

pyrometallurgical operations have been introduced, but these have yielded no sustainable solutions [22]. Therefore, development of alternative sustainable solutions, which are less energy intensive, cost effective, and have the potential to by-pass the existing smelting route is required.

One such solution is bioleaching, whereby microorganisms secrete lixiviant or bioactive agents to solubilize metals from solid metallic fractions like ores [28–33]. Moreover, with the declining ore grades, traditional metallurgical processes are becoming ineffective, whereas microorganisms work well under such circumstances and can easily access metals from low-grade ores [34]. Bioleaching technology has been tried and tested and found to be economical and effective for the extraction of metals such as gold, copper, and nickel from primary and secondary resources using thermophilic or mesophilic microorganisms [29, 35–38]. Compared to mesophiles, thermoacidophilic archaea (e.g., *Sulfolobus* sp., *Metallosphaera* sp., and *Acidianus* sp.) are capable of bioleaching minerals with faster kinetics and greater dissolution efficiency [39–43]. For instance, Norris et al. [44] achieved efficient copper extraction from chalcopyrite with moderate thermophilic bacteria at 50 °C and using thermophilic archaea at up to 80 °C. Moreover, bioleaching operations at large scale can produce a substantial amount of heat (exothermic) [45]; therefore, using thermophilic archaeobacteria can help maintain cell viability (because of their inherent suitability to high temperature), and thereby process efficiency. Studies conducted by different researchers reported higher sphalerite (CuFeS_2) leaching rate using *A. brierleyi* as compared to mesophilic bacterium [46, 47]. Furthermore, species of genus *Sulfolobus* has shown potential to mobilize Cu, Zn, and U, provide desulfurization strategies to coal, and oxidize arsenite to arsenate in culture [43]. Thermoacidophilic *Metallosphaera sedula* feeds its electron transport chain by using various metal-containing ores as well as organic carbon sources [48, 49]. In addition to its inherent capacity for (chalco-) pyrite bioleaching [50], *M. sedula* is also capable of oxidizing solid triuranium octaoxide (U_3O_8) to U(VI) while feeding its own bioenergetic needs [51]. *M. sedula* is also capable of solubilizing precious metals from synthetic as well as extraterrestrial material like meteorites (ordinary chondrite NWA 1172; Martian breccia NWA 7034) [52, 53]. Since individual thermoacidophile archaeobacteria have shown proven bioleaching potential, testing a thermoacidophile consortium might improve process efficiency.

Although the bioprocessing of PGMs is still underdeveloped, the extraction of base metals using microorganisms has been studied by different researchers using Merensky and Platreef ores/concentrates. Mwase et al. [12] studied a two-stage heap bioleaching method for processing low-grade flotation concentrate derived from Platreef ore using microorganisms in bench-scale columns at 65 °C in the

first stage and chemical cyanide (0.1 M, 5 gpl) at 50 °C in the second stage. After 88 days, 91.1% Cu, 98.5% Ni, and 83.5% Co were extracted in the first stage. In the second stage, 96.5% Pd, 97.5% Au, and 35% Pt were extracted using chemical cyanide after 45 days. Mwase et al. [54] also examined a sequential heap bioleaching technique for processing Platreef ore using microorganisms in cylindrical columns, at 65 °C, in the first stage, and chemical cyanide (0.1 M, 5gpl) at 50 °C in the second stage. After 304 days, 93% Cu, 75% Ni, and 53% Co were extracted in the first stage. In the second stage, 57.8% Pt, 99.7% Pd, and 90.3% Au were extracted using chemical cyanide after 60 days. The technique was proposed to treat Platreef ore. Heidrich et al. [55] studied stirred-tank bioleaching of Platreef-oxidized PGE ores at moderately high temperatures using a consortium of iron- and sulfur-oxidizing acidophiles dominated by *Acidithiobacillus caldus* and *Sulfobacillus thermosulfidooxidans*. Bioleaching achieved up to 86% total metal recovery (including Co, Cu, Mn and Ni) in the first stage. In the second stage, up to 89% Pt and 96% Pd were chemically extracted using HNO_3/NaCl and chemical cyanide. In another study, Mwase et al. [19] investigated a heap bioleaching technique for processing concentrator slurry derived from Merensky Reef ore using packed bed columns and a mixed culture of thermophiles and mesophiles at 65 °C in the first stage, and chemical cyanide (0.15 M) at 23 °C in the second stage. After 30 days, 52% Cu, 95% Ni, and 85% Co were extracted in the first stage. In the second stage, 20.3% Pt, 87% Pd, and 46% Rh were extracted using chemical cyanide after 21 days. In the foregoing flowsheets, cyanide was used for PGM leaching. This agrees with Nunan [56] who reported that it is necessary to remove base metals from PGM ore because they lock up PGEs in refractory sulfidic matrices as well as compete with PGEs for cyanide during leaching.

While the bioprocessing of PGMs from the Merensky and Platreef ores has been researched, there is a dearth of information on the bioprocessing of the UG-2 ore/concentrates. Moreover, most of the bioleaching studies were aimed at pre-treatment as a step to concentrate PGEs for subsequent extraction through chemical cyanidation. Presently, there is no known two-stage biological process, in commercial operation, which can completely extract PGEs as well as base metals from PGM ore. Therefore, the present paper gives the results of a fundamental study on the bioleaching of base metals from UG-2 flotation concentrate using a mixture of indigenous thermoacidophile archaeobacteria namely, *Acidianus brierleyi*, *Sulfolobus* sp., and *Metallosphaera sedula*. The primary objective of this study, therefore, was to identify the factors that significantly influence the base metal dissolution from UG-2 flotation concentrates and to optimize the bioleaching conditions. Process optimization was done using a statistical Design of Experiments (DOE) based on the Response Surface Methodology (RSM). Furthermore,

the feasibility of the bioleaching process was evaluated using the continuous stirred-tank reactor. The study represents only part of the work done in a broader investigation to evaluate a completely biological two-stage process for the extraction of base metals, which would otherwise co-extract and interfere if extracted together with PGEs. In this paper, only the first stage of the process is presented.

Materials and Methods

Materials

The UG-2 PGM concentrate used in the experiments was supplied by Eastern Platinum concentrator, Sibanye-Stillwater (Pty) Ltd (formerly, Lonmin (Pty) Ltd), South Africa.

Material Analytical

The mineralogical characterization of the UG-2 PGM material was carried out using Mineral Liberation Analysis (MLA) and Quantitative Evaluation of minerals by Scanning electron microscopy (QEMSCAN), X-ray diffraction (XRD), and X-ray fluorescence (XRF) spectroscopy techniques. Particle size distribution (PSD) was determined by using automated quantitative scanning electron microscopy (A-SEM). The sample was also screened into three screen sizes of $-38\ \mu\text{m}$, $-106\ \mu\text{m} + 38\ \mu\text{m}$, and $+106\ \mu\text{m}$ in line with the DOE plan and analyzed for elemental composition. A pulverized portion was submitted for 6E analysis (Pt, Pd, Rh, Ir, Ru, Au) by fire assay [57] (online supplementary material Table S-1). Major elements (Mg, Fe, Al, Ca, Si, Cu, Pb, Zn, Ni) were analyzed by sample fusion followed by acid digestion [58] in HCl/HNO₃ (Table S-1) and read by Inductively Coupled Plasma-Optical Emission Spectrometry (ICP-OES), with a detection limit $>0.05\ \text{wt}\%$. Bulk mineralogy was conducted by X-ray diffraction using a Bruker D8 Advance instrument. The minerals were identified using the Bruker EVA software and quantified using the Rietveld refinement method with the TOPAS software program. The technique has a typical detection limit of 1 wt%. A base metal sulfide search was conducted using A-SEM (MLA or QEMSCAN) to determine species, liberation, association, and grain size distribution. The PGM search was conducted using a Mineral Liberation Analyzer (MLA) to determine liberation, association, grain size distribution, and species.

Microbial Consortium and Cultivation Conditions

An indigenous consortium containing a mixture of thermoacidophilic archaeobacteria namely, *Acidianus brierleyi*, *Sulfolobus sp.*, and *Metallosphaera sedula* was employed in the bioleaching study. The consortium was sourced from Mintek, South Africa, who, also, are custodians of the

microbial community data on these isolates. The consortium was maintained at 65 °C in Silverman 9 K basal medium consisting of 3 g [NH₄]₂SO₄, 0.1 g KCl, 0.5 g MgSO₄·7H₂O, 0.5 g K₂HPO₄, 0.01 g Ca(NO₃)₂ per liter of distilled water [59] having pH 1.8 and 5% (w/v) sulfur powder. The pre-adapted consortium i.e., adapted to 10% (w/v) solid load, was used as inoculum in the bioleaching tests.

Design of Experiments

Factorial Design

Statistical Design of Experiments (DOE) was employed to study the bioleaching behavior of UG-2 concentrate using a 2⁵ full factorial design. In this study, the choice of factors and levels was based on literature. Experimental design factors were classified as controlled factors and held constant factors. The controlled factors, presented in Table 2, were the factors selected for investigation. The held constant factors such as agitation rate and sulfur substrate are factors that may have an influence on the response, but they were held constant at 150 rpm [60, 61] and 5%, respectively. The choice of 5% sulfur content was based on diagnostic tests carried out prior to running the final experiment. Different sulfur contents were evaluated and the one resulting in most extractions was selected (online supplementary material Fig. S-1).

Methodology for Data Analysis

Normal Probability Plot of Effects

In the assessment of effects from unreplicated factorials, occasionally real and meaningful higher-order interactions occur, and therefore, it is necessary to allow for selection. A normal probability plot method [62] by which effects are plotted was used to provide an effective way of helping with the selection of significant effects.

Response Surface Methodology and Central Composite Rotatable Design

The response Surface Methodology (RSM) was used in this study. The main objective of employing RSM was to optimize the process variables that significantly influence a process [63]. The data for fitting the second-order response was

Table 2 Controlled factors and their levels

Controlled factors	Low (-1)	Center point (0)	High (+1)
1 pH	1.3	1.7	2.0
2 particle size (μm)	-38	$+38-106$	$+106$
3 pulp density (%w/v)	5	10	15
4 inoculum dosage (%v/v)	5	12.5	20
5 temperature (°C)	50	65	80

collected by using the central composite rotatable design (CCRD). The experimental results were analyzed statistically by using the analysis of variance (ANOVA) based on Fisher's ratio test; standard errors of model coefficient (t-test); and the coefficient of determination (R^2). For the five variables under consideration, a second-order polynomial regression model was proposed as follows:

$$y = \beta_o + \sum_{i=1}^5 \beta_i x_i + \sum_{i=1}^5 \beta_{ii} x_i^2 + \sum_{i=1}^5 \sum_{j=i+1}^5 \beta_{ij} x_i x_j + \varepsilon, \quad (1)$$

where y is the predicted response, β_o is the coefficient for intercept, β_i is the coefficient of linear effect, β_{ii} is the coefficient of quadratic effect, β_{ij} is the coefficient of interaction effect, ε is a term that represents other sources of variability not accounted for by the response function; x_i and x_j are coded predictor variables for the independent factors. The coefficients of the regression model were estimated by fitting the experimental results using Design Expert® 11 software.

Experimental

DOE Shake Flask Optimization Tests

The DOE leaching experiments were carried out in 250-mL Erlenmeyer flasks, a thermal shaking incubator, and a filter funnel fitted with filter paper. The filter funnel was mounted on a 1000-mL Erlenmeyer flask connected to a vacuum filtration system. Leaching experiments consisted of adding inoculum, a weighted UG-2 PGM concentrate sample, and 5% sulfur in 100 mL sterilized 9 K basal medium contained in the volumetric flask followed by agitating the slurry in a constant temperature shaking incubator. Sulfur was added to aid the microorganisms' sulfur-oxidizing reactions because UG-2 PGM concentrates are typically characterized by low sulfide content. Separate samples were used for each allotted leaching condition. The leaching was conducted at a constant agitation rate of 150 rpm. The uninoculated control experiments were run in parallel.

CSTR Confirmatory Tests

To confirm the shake flask test results as well as evaluate the industrial applicability of the bioleaching process, confirmatory tests based on optimized conditions were conducted using a continuous stirred-tank reactor (CSTR). A 2-L bioreactor (Sartorius, South Africa) containing 1.5 L medium was operated at 10% (w/v) pulp density in a sterilized 9 K basal medium containing a sterilized 5% sulfur as the energy source and pH was maintained as required using sulfuric acid or NaOH. The CSTR was aseptically inoculated with a pre-adapted microbial consortium and agitated

at 400 rpm for a period of 21 days. To maintain aerobic conditions, the CSTR was sparged with filter-sterilized air, using a 0.45 μm filter and a peristaltic pump (Hei-Flow Core 120, Germany).

Analytical

After leaching, the leached residue was separated from the solution by filtration. The dry solid residue was analyzed by X-ray diffraction (XRD) and the corresponding leach liquor by Inductively Coupled Plasma-Optical Emission Spectrometry (ICP-OES). All experiments were randomly run to "average out" the effects of extraneous factors that may have been present [64]. Redox potential and pH were regularly monitored during leaching, and the latter was controlled periodically using sulfuric acid or NaOH. The pH and redox potential were measured using a standard pH meter (Orion Star™ A211 Benchtop pH Meter-Thermo Fisher Scientific, USA). The redox potential readings were obtained using the Ag/AgCl/4 M KCl reference electrode and subsequently converted to the standard hydrogen electrode (SHE) by adding 228 mV [65]. The concentration of Fe^{2+} in the leach solution was measured by titration using a standardized 0.0165 M potassium dichromate ($\text{K}_2\text{Cr}_2\text{O}_7$) titrant, and the Fe^{3+} was determined by the difference between the titrated Fe^{2+} and the Fe (total). Microbial mass measurements were done as per the protocol described by Li and Orduna [66]. All experiments were carried out in triplicates over a period of 21 days.

Results and Discussion

UG-2 Concentrate Characterization

Particle Size Distribution

The particle size distribution (PSD) of the UG-2 PGM concentrate is shown in Fig. 1. By interpolating the P80 from the

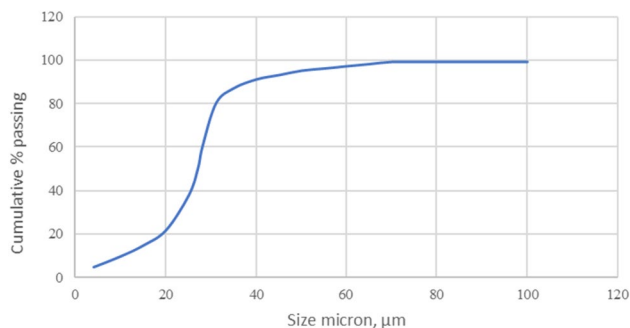


Fig. 1 Cumulative percent passing graph

cumulative percentage passing against sieve size, the graph in the figure below shows that the material's P80 is 32 μm .

Chemical Composition

The chemical composition of the UG-2 PGM flotation concentrate has a high Si content of 21.06 wt%. The content of PGEs in the sample was 119.0 ppm Pt, 72.1 ppm Pd, 23.2 ppm Rh, and 2.18 ppm Au (Table S-2).

Elemental Composition by Particle Size

The elemental composition of the UG-2 PGM flotation concentrate by particle size is presented in Table 3. The results in the table indicate a marked grade range. The smaller particles had a lower grade compared to the larger size. This may have been caused by the tendency for flotation to be non-selective at smaller particle sizes, thus, resulting in gangue entrainment and decreased concentrate grade [67].

Bulk Mineralogy

The bulk modal analysis of UG-2 PGM flotation concentrate (Table S-3) is composed of major amounts of pyroxene (41.8wt%), talc (16.7wt%), mica (13.0wt%), serpentine (11.5wt%), and chromite (4.2wt%). Amphibole, chlorite, pentlandite, chalcocopyrite, pyrite, and feldspar are in trace amounts. Geologically, the primary sulfide minerals associated with PGMs are pyrrhotite, chalcocopyrite, pentlandite, and pyrite, and the rest are gangue minerals [4].

Base Metal Sulfides

The base metal sulfide analysis (Table S-4) shows that the material is composed of major amounts of pentlandite (41.3%), chalcocopyrite (25.7%), pyrrhotite (19.5%), pyrite (12.2%), and trace amounts of millerite and other base metal sulfides. The BMS grain size distribution (Table S-5) shows that 58.5% BMS grains are fine size (< 20 μm), 26.2% are of medium size (20–50 μm), and 15.3% are coarse (> 50 μm). The BMS grain mode of occurrence (Tables S-6 and S-7) shows that the

liberation of the BMS, in the context of both free surface and area % liberation is high. Pentlandite, chalcocopyrite, and pyrrhotite have cumulative liberations of 92.3%, 88.4%, and 87.6% respectively. The high degree of liberation indicates that BMS may be particularly amenable to removal from the UG-2 PGM flotation concentrate. The base metal sulfide minerals (Table S-8) namely pentlandite, millerite, chalcocopyrite, pyrrhotite, and pyrite are highly associated with each other.

PGM

The distribution of PGM mineral species (Table S-9) shows that PGEs are hosted within numerous phases and the most significant contributors include (Pt, Pd)S (47.1%), PtS (19.6%), PtAs (13.6%), PtRhCuS (8.6%), and PtFe (2.1%). The PGM grain size distribution (Table S-10) shows that 23.9% of PGM grains are fine size (< 20 μm) and 76.1% are medium (20–50 μm) size. The coarse size (> 50 μm) does not contain PGMs. The PGM grain mode of occurrence (Table S-11) shows that 50.1% of the PGMs are liberated, 33.6% are associated with liberated base metal sulfides, 10.2% are associated with base metal sulfides attached to silicate and oxide gangue particles, 4.4% are attached to silicate and oxide gangue particles, and 1.6% are locked within silicate and oxide gangue particles. The strong association of PGMs with BMS suggests that there needs to be a consideration in the context of discrete processing routes for base metals and PGEs. The presence of base metals in PGM ore presents a challenge because they lock up PGEs in refractory sulfidic matrices as well as compete with PGEs for cyanide, thus, adversely affecting PGE recoveries and causing high cyanide consumption [54]. For this reason, a base metal extraction process prior to PGE recovery is essential [9].

Significant Factors

The base metal extractions were calculated as a percentage of the base metal in leach liquor to that in the unprocessed UG-2 PGM concentrate. The experimental data obtained from the DOE screening tests was used to estimate the main and interaction effects on the normal probability plot (Fig. S-2), which was also used to determine the significant effects. The statistically significant main factors were identified as pH, pulp density, inoculum dosage, and temperature as well as their interactions.

Influence of Factors on Base Metal Extraction

Variables may be individually interpreted only if there is no evidence of interaction among each other else the interacting variables should be considered jointly [68]. In this study, the main factors and factor interactions were statistically significant. Therefore, all the main factors were first interpreted individually, and the interacting variables, jointly.

Table 3 Elemental compositions of UG-2 PGM concentrate by particle size

Element (wt. %)	Co	Cr	Cu	Fe	Ni
-38 μm	0.048	1.018	0.587	9.14	1.471
+38–106 μm	0.057	1.100	0.794	9.75	1.799
+106 μm	0.076	1.224	1.677	11.9	2.506

Effect of pH

The concentration of hydronium ions is an important factor for the effective bio-dissolution of metals by proton attack. To investigate the effect of pH, DOE experiments were carried out at pH levels of 1.3 and 2.0. Results in Fig. 2 show that higher pH favored Co, Cu, and Ni extraction while lower pH promoted Cr and Fe extraction. Previous studies have reported that proton concentration is not a single key factor for bioleaching but rather part of a complex interaction between microorganisms and redox potential, metal ions, and protons operating close to the mineral surface [69]. In spite of not being the only key factor, protons generated by microorganism catalytic activity seem to have played a major role in influencing Co, Cu, and Ni extraction. A possible formation of precipitates at high pH may have adversely affected mass transfer rates for Cr and Fe, thus, decreasing their extraction efficiency.

Effect of Particle Size

Particle size defines the contact surfaces that affect mass transfer and collision between particles and microorganisms,

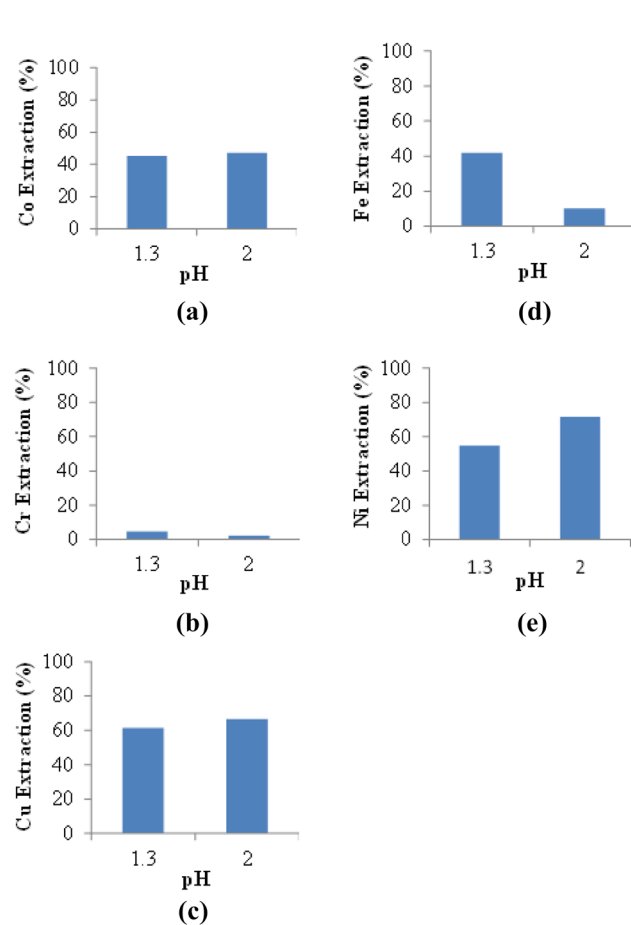


Fig. 2 a–e: Effect of low and high pH on base metal extraction

which in turn affects the activity of the microorganisms [70]. To examine the effect of particle size, experiments were conducted at particle sizes of $-38 \mu\text{m}$ and $+106 \mu\text{m}$. Although the large particle size in the size-by-size analysis (Table 3) was observed to have a higher grade, results in Fig. 3 show that metal recovery was most efficient at the smaller particle size for Co, Fe, and Ni, except Cu. Similar findings in previous bioleaching studies are reported by Nemati et al. [71], and Hedrich et al. [55]. As observed by Vera et al. [69], bioleaching is a complex interaction between microbial cells operating close to the mineral surface. Therefore, the efficient metal recoveries at smaller particle sizes could be attributed to better mass transfer and faster reaction kinetics due to better microorganism contact on larger surface areas.

Effect of Pulp Density

To study the effect of pulp density, experiments were carried out at pulp densities of 5% (w/v) and 15% (w/v). The results in Fig. 4 show that a lower pulp density enhanced metal dissolution for all the five base metals studied.

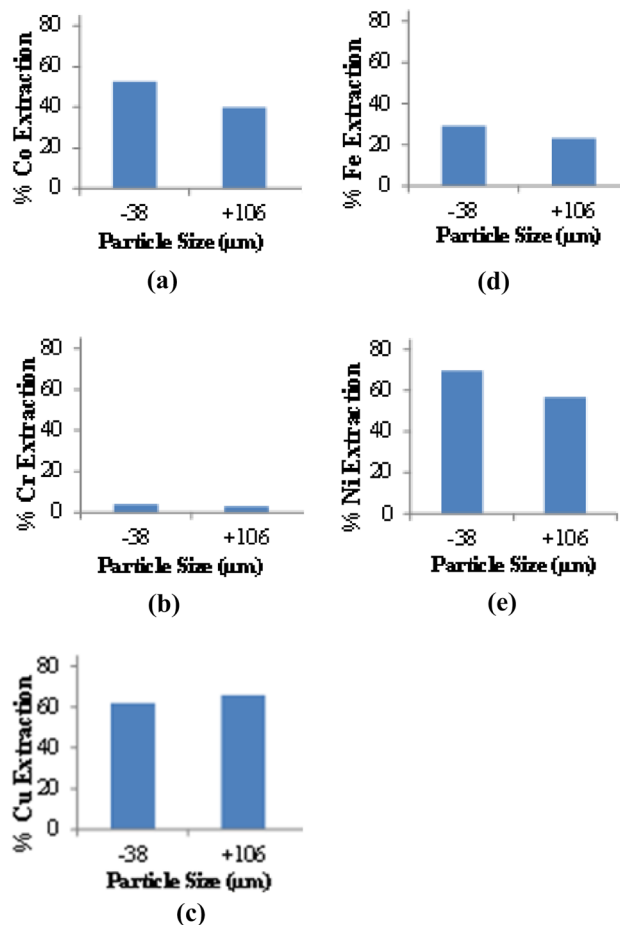


Fig. 3 Effect of small and large particle size on base metal extraction

Lower pulp density allows for a less dense slurry mixture, and frees up solid particles, hence, optimizing available surface area for microorganism contact [69]. A larger available surface area for contact, in heterogeneous systems, leads to higher reaction rates. The negative effect of high pulp densities was reported by Torma et al. [72, 73] when bioleaching with thermophilic bacteria. The authors observed that, at high slurry densities, bacterial microorganisms are susceptible to mechanical damage and metabolic stress caused by the intense agitation needed to maintain a homogeneous suspension [74–77].

Effect of Dosages of Bacterial Inoculum

To explore the effect of inoculum dosage, experiments were conducted at inoculum dosages of 5% (v/v) and 20% (v/v). Results presented in Fig. 5 show enhanced metal dissolution at higher inoculum dosage for all metals except Cr suggesting that increased inoculum dosage had a positive impact. Higher inoculum dosage may have increased the capacity for the metal–microbe interaction and enhanced

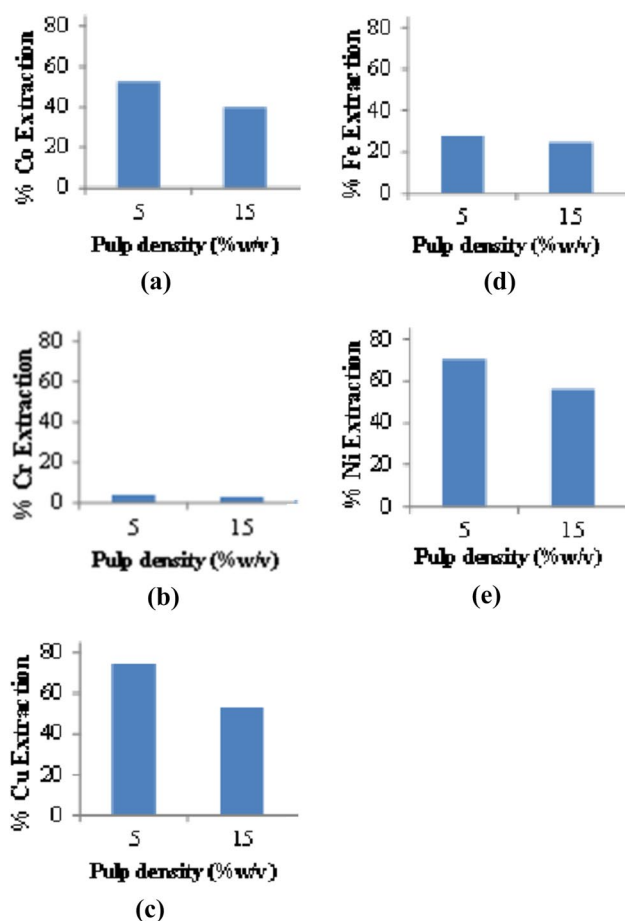


Fig. 4 Effect of low and high pulp density on base metal extraction

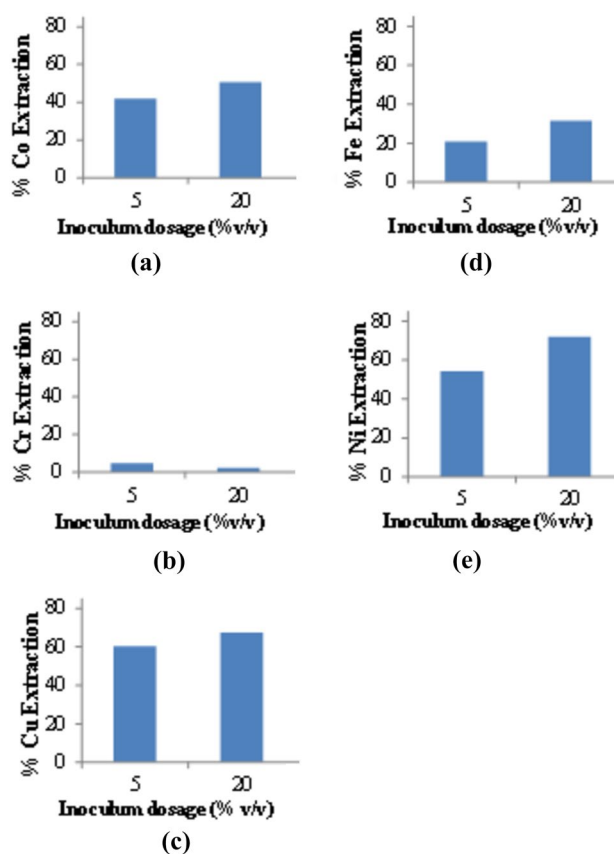


Fig. 5 Effect of inoculum dosage on base metal extraction

lixiviant production, which in turn promoted metal extraction efficiency. The low Cr extraction at high inoculum dosage could be attributed to the precipitation of metal sulfates that form passivating boundary layers on chromite surfaces. The formation of precipitates which typically include $\text{Fe}_2(\text{SO}_4)_3$, MgSO_4 , and $\text{Cr}_2(\text{SO}_4)_3$ have been reported elsewhere [78–80].

Effect of Temperature

Process temperature enhances reaction kinetics. Temperature also influences the performance of microorganisms because they are temperature-sensitive creatures. To study the effect of temperature, experiments were carried out at 50 °C and 80 °C. Results exhibited in Fig. 6 show that higher temperature promoted metal extraction for all the five base metals studied. The biggest impact was observed on Cu, Ni, Co, and Fe and the least on Cr. As opposed to mesophilic strains, extreme thermophilic bacteria used in this study thrive better at high temperatures of 60–80 °C [81]. Therefore, the high extraction results at high temperature are indicative of better thermophilic microorganism catalytic activity enabled by a high-temperature environment.

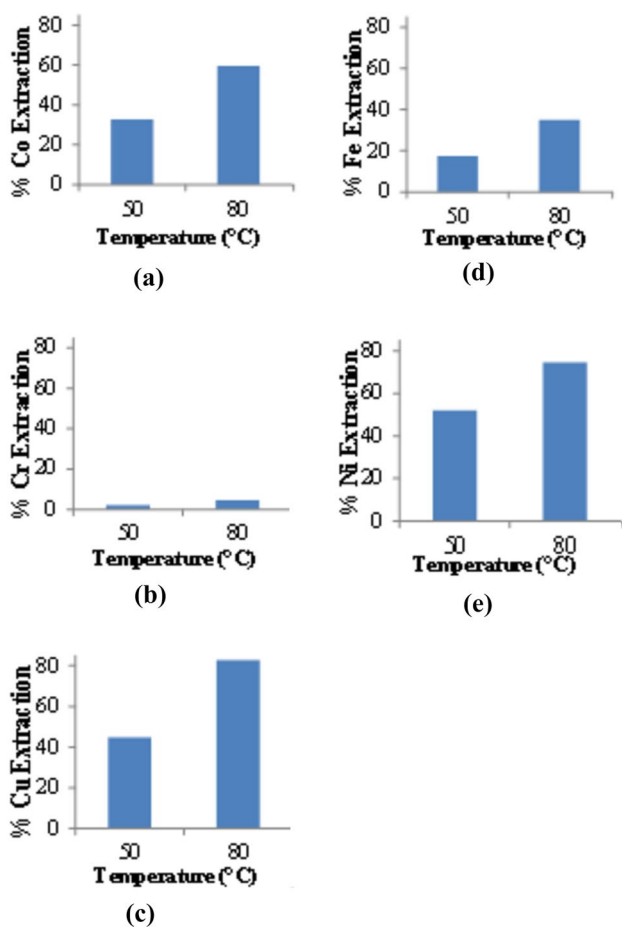


Fig. 6 a–e: Effect of temperature on base metal extraction

Factor Interaction

Factor interaction is a relationship where the effect that a factor has on a product or process is altered due to the presence of one or more factors. The factor interactions noted to have a significant influence on bioleaching the base metals are listed

Table 4 Summary of factor interactions

Element	Main significant factor					Significant factor interaction
	A pH	B Particle size	C Pulp density	D Inoculum dosage	E Temp	
Co		✓	✓		✓	AE
Cr	✓			✓	✓	AE, ADE
Cu			✓		✓	AE, BC
Fe	✓			✓	✓	AE
Ni	✓	✓	✓	✓	✓	AE, BC, DE, CE

in Table 4. Temperature and pH were the key factor interactions for Co; pH, inoculum dosage, and temperature for Cr; pH, particle size, and pulp density for Cu; pH and temperature for Fe. And for Ni, the significant interactions were pH and temperature, particle size and pulp density, inoculum dosage and temperature, and pulp density and temperature.

The base metal sulfide grain mode of occurrence shown in Tables S-6 and S-7 shows that the liberation of base metal elements, in the context of both free surface and area % liberation, is high. Pentlandite, chalcopyrite, and pyrrhotite have cumulative liberations of 92.3%, 88.4%, and 87.6%, respectively. This high degree of liberation indicates that base metals were particularly amenable to removal from the UG-2 PGM flotation concentrate during the leaching process. The high degree of base metal liberation, therefore, plays a key role in the extraction of the Co, Cu, Ni, Fe and Cr base metals.

Optimization of Significant Factors

Among the four significant factors identified in Sect. “Significant factors,” pH, pulp density, and inoculum dosage were selected for optimization studies. The temperature factor was held constant at 80 °C in accordance with the nature of thermophilic microorganisms. Based on quadratic programming, RSM in conjunction with CCRD was used for deriving a regression model, which in turn was employed in modeling optimal conditions.

Derivation of the Fitted Model

The experimental results (Table S-12) were collected by using CCRD. The results were used for fitting the second-order response and estimating the coefficients of the regression model. The fitted second-order models for Co, Cr, Cu, Fe and Ni were as follows:

$$Y_{\text{Co}} = 44 - 3.22x_1 - 13.71x_2 - 3.67x_1x_2 + 4.46x_1x_3 - 4.31x_2x_3 + 4.27x_2^2 - 3.17x_3^2 + 3x_1x_2x_3 + 18.56x_1^2x_2, \quad (2)$$

$$Y_{\text{Cr}} = 2.37 - 1.38x_1 - 1.98x_2 - 0.40x_1x_2 + 0.46x_1x_3 - 0.84x_2x_3 + 0.41x_1^2 + 0.93x_2^2 + 0.38x_1x_2x_3 + 1.64x_1^2x_2 - 0.32x_1x_2^2, \quad (3)$$

$$Y_{\text{Cu}} = 56.55 - 6.90x_1 - 16.11x_2^2 - 8.61x_1x_2 + 4.98x_1x_3 - 7.67x_2x_3 + 5.29x_2 - 3.71x_3^2 + 5.24x_1x_2x_3 + 25.45x_1^2x_2^2, \quad (4)$$

$$Y_{\text{Fe}} = 1.18 - 0.48x_1 - 2.02x_2 + 0.13x_3 + 0.17x_1x_3 - 0.40x_2x_3 + 0.15x_1^2 + 1.06x_2^2 + 1.61x_1^2x_2 - 0.46x_1^2x_2^2, \quad (5)$$

$$Y_{\text{Ni}} = 41.39 - 24.8x_1 - 10.65x_2 - 3.64x_1x_2 + 4.09x_1x_3 - 3.92x_2x_3 + 2.94x_2^2 - 2.74x_3^2 + 15.52x_1^2x_2, \quad (6)$$

where, x_1 = pH, x_2 = pulp density, and x_3 = inoculum dosage, within predictor variable limits:

$$-\lambda \leq x_i \leq +\lambda; i = 1, 2, 3,$$

x_i are coded predictor variables and $\lambda = 2^{(k-q)/4} = 1.682$ (for $k=3, q=0$) is the distance of the axial points from the center of the CCRD that gives the limits of the valid region under experimentation.

Checking the Adequacy of the Fitted Model

The adequacy of the fitted second-order models was checked using the analysis of variance (ANOVA) at a statistical significance confidence level limit of 95%. The models were found to be significant and did not present any evidence of a lack of fit. The quadratic and interactive terms were found to be insignificant. The relationship between experimental and predicted metal extractions (Fig. S-3) showed that predicted values were reasonably comparable to the experimental values. Linear correlation coefficients (R^2) of 92.5% for

Co, 99.3% for Cr, 93.2% for Cu, 97.3% for Fe, and 88.0% for Ni verified the fitness of the models. Statistically, this means 92.5%, 99.3%, 93.2%, 97.3%, and 88.0% of the sample variation for Co, Cr, Cu, Fe, and Ni, respectively, could be explained by the independent variables.

Determination of Optimum Conditions

The optimization of the three significant factors was numerically evaluated by setting optimization criteria for the variable factors and the response. The optimum factor levels for each metal were averaged and then pertinent levels were determined (Table 5). The optimal base metal bioleaching conditions were 1.3 pH, 10% (w/v) pulp density, 18% (v/v) inoculum dosage, 80 °C temperature, 400 rpm agitation rate, and 21 days residence time. Although the bioleaching experiment was allowed to run for 21 days, the data shows that a reaction time of about 16 days was suitable for leaching Co and Ni base metals.

The 21-day residence time reported in the current study is relatively long compared to what is found in industry practice. However, it must be noted that the leaching conditions for base metals extraction from PGM concentrates used in industry are relatively harsher (see Table 8), hence, the shorter industry residence time. Industry uses high pressure oxidation (POX) and high temperatures in the range of 150–225 °C [82] whereas the bioprocess in the current study was performed under atmospheric conditions and a relatively lower temperature of 80 °C. On the other hand, a study by Heidrich et al. [55] leached chalcopyrite using moderately thermophilic acidophiles in a stirred-tank reactor and extracted 86–97% Cu at 65 °C in 10 days. It should be noted, however that the sample used in their study was a near-surface-oxidized PGE ore, which is different from the refractory sulfide mineral used in this study.

Using Eqs. 2–6, the predicted extractions were

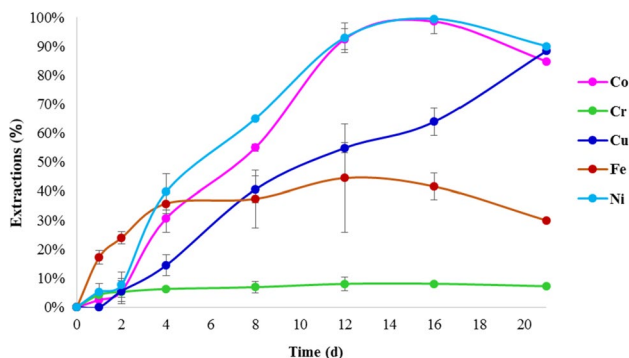
Co, = 92%; Cr, = 6%; Cu, = 97%; Fe, = 20%; Ni, = 99%.

Table 5 Summary of optimum factors

Element	A pH	C pulp density %(w/v)	D inoculum dosage %(v/v)
Co	1.3	12	15
Cr	1.5	5	24
Cu	1.7	12	15
Fe	1.3	5	20
Ni	1.7	12	15
Avg	1.5	9.2	17.8
Pertinent	1.3	10	18

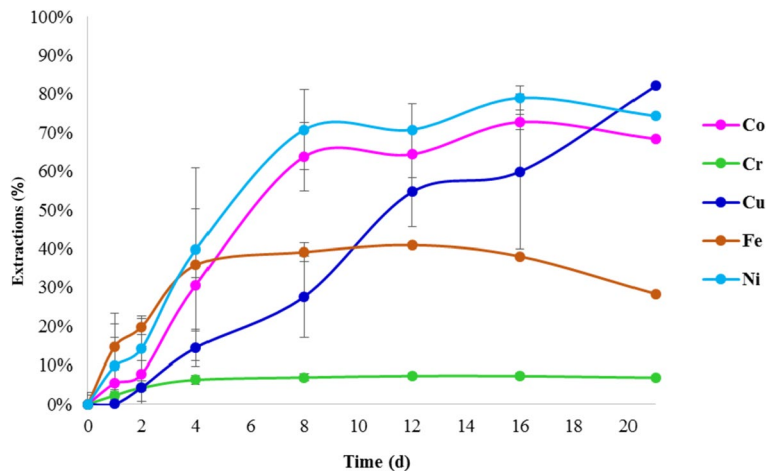
Table 6 Base metal extractions at optimum leaching conditions

Parameter	pH	Pulp density %(w/v)	Inoculum dosage %(v/v)	% Extraction				
				Co	Cr	Cu	Fe	Ni
Model	1.3	10	18	92	6	97	20	99
Confirmatory tests	1.3	10	18	99.3	8.1	90.1	41.6	99.5

**Fig. 7** Base metal extraction profile conducted in the presence of microorganisms.

Confirmatory Experiments

To test the validity of the modeled optimum shake flask bioleaching conditions, CSTR tests were carried out using parameters suggested by the model (Table 5) and the confirmatory test results obtained are shown in Table 6. The confirmatory test results for Co, Cr, Cu, and Ni were found to be consistent with the model and, therefore, considered to fit the experimental data well. Iron was not consistent with the model probably due to its precipitative behavior under these leaching conditions.

Fig. 8 Base metal extraction profile conducted in the absence of microorganisms

Confirmatory Experiment Extraction Profiles

Extraction profiles obtained at optimum conditions for Co, Cr, Cu, Fe, and Ni are presented in Fig. 7. The figure shows a maximum extraction of 99.5% for Ni, 99.3% for Co, 41.58% for Fe, and 8.1% for Cr on day 14. A maximum extraction of 90.1% for Cu occurred on day 21. The extraction efficiency for Fe shows a decreasing trend beyond day 14 suggesting predominance in Fe precipitative reactions and formation of jarosite [83, 84]. Except for Cu, the corresponding decline in Ni and Co extraction could be associated with jarosite formation. Similar findings were reported by Mamindy-Pajany et al. [85] who suggested that jarosite has adsorptive properties for base metals. Despite being the most abundant among the five base metals, Fe was the second least extracted after Cr. Fe exists predominantly in the refractory sulfidic phase as pentlandite, chalcopyrite, pyrrhotite, and pyrite. Cr is present in the chromite phase. The Fe and Cr phases are resistant to dissolution due to strong passive behavior in acid solutions [86]. Similar patterns for chromium and its formation of insoluble metal sulfates are consistent with findings elsewhere [78, 80, 87, 88].

Control Experiment Extraction Profiles

Extraction profiles obtained for control tests performed in the absence of microorganisms are shown in Fig. 8. The figure shows 79% extraction for Ni, 73% for Co, 60% for Cu, 38% for Fe, and 7% for Cr, on day 16. While maximum

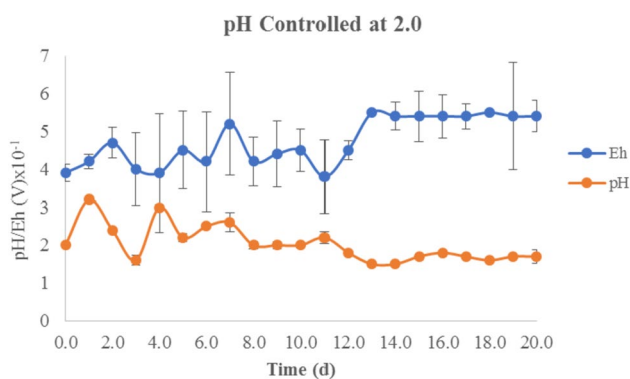


Fig. 9 pH and Eh trend with pH control

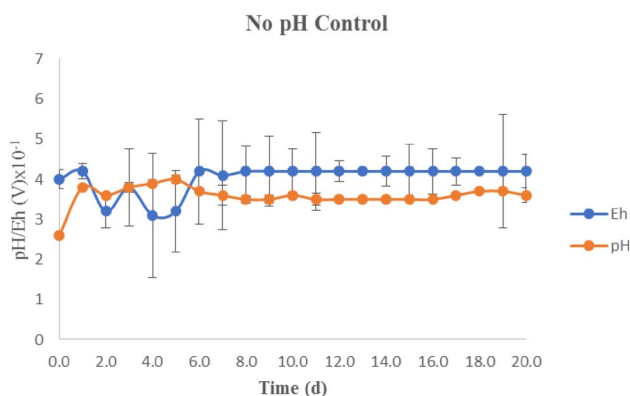


Fig. 10 pH and Eh trend without pH control

metal extraction in control tests occurred on day 16, for the bioleaching tests, it occurred on day 14, suggesting that bioleaching was much more efficient. While Cu extraction increased to 82.1% on day 21 in control tests, for the bioleaching test, the extraction was 90.1%, thus, 8% higher.

In general, the relatively lower extractions in the control experiment could be attributed to the fact that PGM sulfidic

material is refractory and difficult to leach without a mechanism to catalyze the breaking down of the sulfidic matrix that houses the base metal sulfides. This indicates that metal extraction in the bioleaching system was enhanced by the presence of sulfur-oxidizing microorganisms' ability to catalyze the breaking down of the refractory sulfidic matrix.

Eh, pH, Fe, and Microbial Biomass Profiles

To study the pH and Eh trend, experiments were conducted for 21 days with and without pH control. The pH and Eh trend in Fig. 9 show much variability in the first 15 days and then stabilize thereafter. The pH variability is attributed to dissolution reactions by Ni, Fe, and Co, which is associated with the steady rise in reaction rates for these elements as shown in Fig. 7, within this same residence time.

The pH profile in Fig. 10 where there was no pH control shows a steep initial rise of pH from 2.6 to 4.1 and less variability after day 5. The initial pH rise is attributed to hydronium ion-depleting metal dissolution reactions. The hydronium ion depletion, however, seems to be moderated by reactions of sulfides producing acid, though mildly because the UG-2 PGM concentrates do not have much sulfur content. The need to keep the pH low and close to the recommended value of 1.3 is evident in Figs. 9 and 10, hence, the need for sulfur supplementation.

The $\text{Fe}^{2+}/\text{Fe}^{3+}$ profile in Fig. 11 is indicative of a strongly oxidizing environment in which Fe^{2+} undergoes oxidation to Fe^{3+} . Usually, Fe (II) and Fe (III) in solution are measured in bioleaching studies to reveal Fe (II) oxidizing activity. The changes in the redox potential, as presented in Figs. 9 and 10 and changes in the $\text{Fe}^{2+}/\text{Fe}^{3+}$ ratio as shown in Fig. 11, are an indication of Fe (II) microorganism oxidizing activity in the base metal bioleaching system. The upward trend in the $\text{Fe}^{2+}/\text{Fe}^{3+}$ ratio after day 8 (200 h) suggests that Fe^{3+} may have started decreasing due to the formation of jarosite precipitates (Table 7), under these leaching conditions, as observed in Figs. 7 and 8.

Fig. 11 $\text{Fe}^{2+}/\text{Fe}^{3+}$ ratio showing Fe^{2+} depletion and Fe^{3+} accumulation with increasing residence time

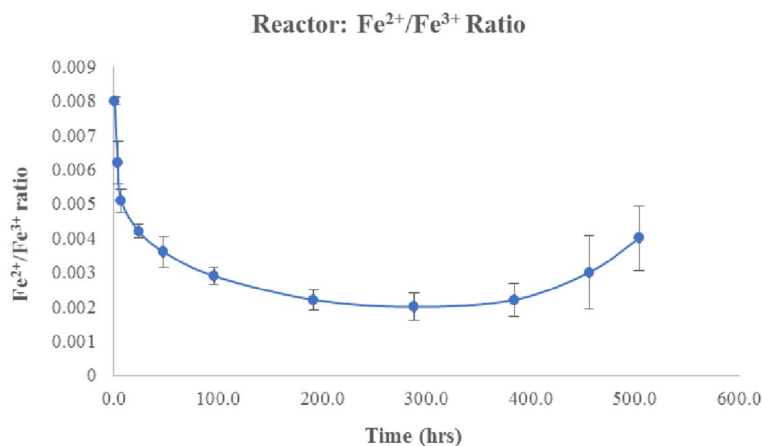
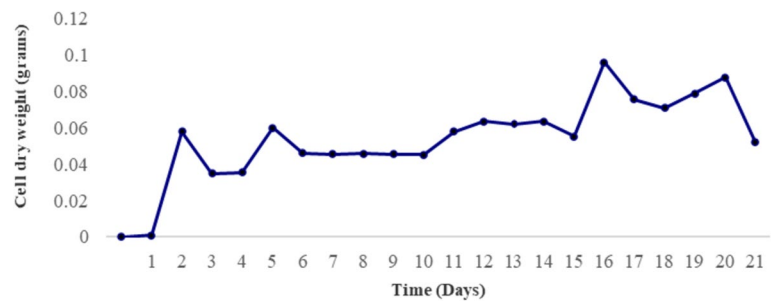


Fig. 12 Cell dry weight, samples taken daily and dried at 66 °C, weight measured every 24 h



The profile for change in microbial biomass over a 21-day period (Fig. 12) shows an increasing trend. A slight decline was observed on days 18 and 21. Microbial biomass in soil has been shown to be affected by the parent material, pH, and organic matter [66]. In the current study, the changes in biomass are postulated to have been caused by the changing composition of the parent material (UG-2 PGM concentrate) as the pH was kept consistent from day 1 to day 21.

Impact of Bioleaching on UG-2 PGM Concentrate Phase Mineralogy

Changes in the UG-2 PGM concentrate phase mineralogy before and after bioleaching are presented in Table 7. The disappearance of augite, hornblende, anorthite, lizardite, biotite, clinocllore, chromite, and pyrite after bioleaching could be attributed to dissolution reactions. The elemental sulfur observed in the pre-treatment residue is the excess sulfur, which was not utilized by the microbes during leaching. A similar phenomenon was also reported by Hedrich et al. [55]. The appearance of jarosite, actinolite, muscovite, diopside, and brucite, after bioleaching suggests precipitative reactions during leaching. Via a hydration mechanism, the MgO present in the PGM concentrate may have been hydrated during leaching to produce Mg (OH)₂ in the form of magnesia gel or crystalline brucite [89]. The presence of diopside and actinolite after bioleaching indicates that tremolite, a member of the amphibole group of silicate minerals underwent conversion under high-temperature (~80 °C) conditions to form new phases [90]. The presence of muscovite, a hydrated phyllosilicate mineral of aluminum and potassium [91] indicates that the mica group of minerals underwent a hydration mechanism, during leaching, to form new phases.

Implications of Bioleaching UG-2 PGM Flotation Concentrate

Industry practice for PGM processing is either directly hydrometallurgical or via a pyrometallurgical route. The

hydrometallurgical Kell process [82, 92] is typically a chlorination route, which entails base metal and sulfur removal by pressure oxidation, roasting of the resulting residue at 800–1000 °C, followed by recovery of PGEs by chlorination. The chlorination route is energy intensive and associated with environmental pollution concerns. The pyrometallurgical route involves smelting, converting [7], and processing the converter matte in a base metal refinery for extraction of Ni and Cu [7, 93] followed by processing of PGM residue to recover individual PGEs [7]. The smelter route is energy intensive and equally associated with environmental pollution concerns. Furthermore, the inherent high chrome grades have fundamentally rendered UG-2 concentrates unattractive and difficult to process using the current PGM smelting methods [22]. What is evident, however, is that both the hydrometallurgical and smelting routes are faced with the need to remove base metals to avoid co-extraction of PGEs with base metals. It is known that when cyanide is used for PGE recovery, the presence of base metals competes with PGEs for cyanide, thus, causing poor recoveries and high cyanide consumption [67]. Noting that a significant portion of PGEs are locked in the base metal's sulfide matrices, a base metal recovery process prior to cyanide leaching is, therefore, essential [9].

In the current study, the bioleaching and removal of base metals from UG-2 PGM concentrate was carried out as a pre-treatment process and results show that substantial extraction of base metals from the UG-2 PGM concentrate was successfully achieved. The pre-treatment has the advantage of exposing and freeing PGEs associated with base metals thereby making them available for subsequent extraction. The bio-pre-treatment experiment results have also shown that, while the PGE mainly stayed in the pre-treatment residue, high extractions of base metals are attainable suggesting a potentially feasible option for industrial bioprocessing of the UG-2 PGM flotation concentrate. Thus, the PGE-enriched residue can be further subjected to subsequent bioleaching of PGEs as the second stage of the bioprocess.

A comparison of the current bioprocess with typical industry practice, which by-passes pyrometallurgical pre-treatment, is displayed in Table 8. The key aspects shown in the table are that industry uses pressure oxidation leaching (POX) and high

Table 7 Phase mineralogy of PGM concentrate before and after bioleaching as determined by XRD

Phase	Chemical formula	Before (wt.%)	After (wt.%)
Enstatite/Ferrosilite	(MgFe)SiO ₃	33.1	28.7
Augite	(Ca, Na)(Mg, Fe, Al, Ti)(Si, Al) ₂ O ₆	8.7	–
Hornblende	(Ca, Na) ₂ (Mg, Fe, Al) ₅ (Al, Si) ₈ O ₂₂ (OH) ₂	4.1	–
Anorthite	CaAl ₂ Si ₂ O ₈	<1	–
Lizardite	Mg ₃ Si ₂ O ₅ (OH) ₄	11.5	–
Biotite	K(Mg, Fe) ₃ AlSi ₃ O ₁₀ (F, OH) ₂	13.0	–
Clinocllore	(Mg, Fe) ₅ Al(Si ₃ Al)O ₁₀ (OH) ₈	3.0	–
Talc	Mg ₃ Si ₄ O ₁₀ (OH) ₂	6.7	43.5
Chromite	FeCr ₂ O ₄	4.2	–
Pentlandite	(Fe, Ni) ₉ S ₈	2.8	0.23
Chalcopyrite	CuFeS ₂	1.3	–
Pyrite	FeS ₂	<1	–
Sulfur	S	–	18.5
Jarosite	KFe ₃ (SO ₄) ₂ (OH) ₆	–	6.9
Actinolite	Ca ₂ (Mg _{4.5–2.5} Fe ²⁺ _{0.5–2.5})Si ₈ O ₂₂ (OH) ₂	–	0.35
Muscovite	(KF) ₂ (Al ₂ O ₃) ₃ (SiO ₂) ₆ (H ₂ O)	–	1.15
Diopside	CaMgSi ₂ O ₆	–	0.45
Brucite	Mg(OH) ₂	–	0.22
	Total	100.0	100.0

Table 8 Typical industry chemical leaching of base metals from PGM concentrates [92]

Parameter	Temperature	% Extraction			
		Co	Cu	Fe	Ni
Bioleaching (current study)-atmospheric	80 °C	99.3	90.1	41.58	99.5
POX-mild temp	150 °C	63.4	65.0	72.8	82.4
POX + atmospheric	200 °C	76.4	85.9	68.0	98.1
POX-high temp	225 °C	97.7	98.9	19.8	98.3

POX pressure oxidation

temperature (150–225 °C) [92] whereas the bioprocess in the current study was performed under atmospheric conditions in the presence of microorganisms at a relatively lower temperature of 80 °C. Evidently, the bioleaching system gave better extractions for Co, Cu, and Ni compared to typical industry recoveries at all three temperature and pressure levels. It is worth noting that the Cu recovery in the bioleaching system outperformed the industry system at two temperature levels except at 225 °C. Overall, the bioleaching system showed better performance compared to current industry practice. Also, the bioprocess system has the economic advantage that it has relatively low energy requirements.

Conclusions

By using a combination of the full 2⁵ factorial design and the RSM in conjunction with the CCRD, factors that influence the bioleaching of base metals from UG-2 PGM flotation concentrate using a thermophilic microorganism consortium were identified and optimized.

Pulp density, pH, inoculum dosage, and temperature were found to have more influence in the base metal bioleaching process than particle size. Analysis of the data showed that interaction among factors had a significant influence on the base metal bioleaching process. This implies that the effect that each factor had on the bioleaching process was significantly altered due to the presence of the other factors.

From the prediction model, optimal extraction efficiencies of 92% for Co, 97% for Cu, and 99% for Ni were predicted at optimal values of 1.3 pH, 10% (w/v) pulp density, 18% (v/v) inoculum dosage, 80 °C temperature, 21 days residence time, and 400 rpm agitation rate using a mixture of indigenous thermophilic archaeobacteria namely, *Acidianus brierleyi*, *Sulfolobus* sp., and *Metallosphaera sedula*. A confirmatory test showed extractions of 99.3% for Co, 90.1% for Cu, and 99.5% for Ni, giving an error margin of 0.2%, with linear correlation coefficients of 92.5%, 93.2%, and 88.0% for Co, Cu, and Ni, respectively, hence, verifying the fitness of the model and experimental data.

The results showed a substantial extraction of base metals from UG-2 PGM flotation concentrate suggesting a potentially feasible option for industrial bioprocessing of PGM concentrate.

Recommendations

To establish the practical feasibility and sustainability of the bioleaching of PGMs from UG-2 concentrate, an acid and energy balance across the bioleaching system is highly recommended. Furthermore, research needs to be conducted to optimize the long residence time required for bioleaching using CSTRs. In particular, a techno-economic analysis of the overall bioprocess should be undertaken. This techno-economic evaluation should also pay attention to the energy used (a factor of residence time) in this bioprocess and compare with the energy consumption in the current industry processes.

Supplementary Information The online version contains supplementary material available at <https://doi.org/10.1007/s40831-024-00800-x>.

Acknowledgements The authors would like to thank Sibanye-Stillwater Pty (Ltd) for the PGM samples and Mintek for supplying the indigenous microorganisms used in the study.

Author Contributions Conceptualization, AS, LC, KR, GS, and SN; Funding acquisition, SN; Supervision, SN; Writing—original draft, AS, LC, SN; Methodology, AS, LC, SM, SN; Editing and re-writing, AS, LC, CSY, AK, and SN. All authors have read and agreed to the published version of the manuscript.

Funding Open access funding provided by University of the Witwatersrand. This paper is based on the work funded by the EU Horizon 2020 BIORECOVER Project Number 821096. Two of the authors were funded by the National Research Foundation (NRF Grant Number: 98350) and the Department of Science and Innovation (DSI) funded SARChI chair in South Africa.

Declarations

Conflicts of interest The authors declare no conflict of interest.

Open Access This article is licensed under a Creative Commons Attribution 4.0 International License, which permits use, sharing, adaptation, distribution and reproduction in any medium or format, as long as you give appropriate credit to the original author(s) and the source, provide a link to the Creative Commons licence, and indicate if changes were made. The images or other third party material in this article are included in the article's Creative Commons licence, unless indicated otherwise in a credit line to the material. If material is not included in the article's Creative Commons licence and your intended use is not permitted by statutory regulation or exceeds the permitted use, you will need to obtain permission directly from the copyright holder. To view a copy of this licence, visit <http://creativecommons.org/licenses/by/4.0/>.

References


1. Yakoumis I, Moschovi AM, Panou M et al (2021) Recovery of platinum group metals from spent automotive catalysts: a review. *Clea Eng Technol* 3:100112
2. Oberthür T, Junge M, Rudashevsky N et al (2016) Platinum-group minerals in the LG and MG chromitites of the eastern Bushveld Complex. *South Africa Mineral Deposita* 51:71–87
3. Junge M, Oberthür T, Kraemer D et al (2019) Distribution of platinum-group elements in pristine and near-surface oxidized Platreef ore and the variation along strike, northern Bushveld Complex. *South Africa Mineral Deposita* 54:885–912
4. Thethwayo BM (2018) Extraction of Platinum Group Metals. IntechOpen, London
5. Ndlovu J (2021) Overview of PGM Processing. Anglo Platinum. Available online: <http://www.angloamericanplatinum.com/-/media/Files/A/Anglo-American-Platinum/investor-presentation>.
6. Shaw A, De Villiers LPVS, Hundermark RJ, et al (2013) Challenges and solutions in PGM furnace operation: high matte temperature and copper cooler corrosion. *J S. Afr Institute Mining Metal*, vol. 113(3).
7. Jones RT (2005) An overview of Southern African PGM smelting. Nickel and Cobalt 2005: Challenges in Extraction and Production, pp.147–178
8. Jones RT (1999) Platinum smelting in South Africa. *S Afr J Sci* 95:525–534
9. Schouwstra RP, Kinloch ED, Lee CA (2000) A Short Geological Review of the Bushveld Complex. *Platin Met Rev* 44(1):33–39
10. Seymour RJ, O'Farrelly JI (2001) Platinum Group Metals Kirk-Othmer Encyclopedia of Chemical Technology-Online. Retrieved: 13 September, 2023, from <http://www.mrw.interscience.wiley.com/emrw/9780471238966/kirk/articleplatseym.a01/current/pdf2001>
11. Penberthy CJ, Oosthuizen EJ, Merkle RKW (2000) The recovery of platinum-group elements from the UG-2 chromitite—a mineralogical perspective. *Mineral Petrol* 68:213–222
12. Mwase JM, Petersen J, Eksteen JJ (2012) A conceptual flowsheet for heap leaching of platinum group metals (PGMs) from a low-grade ore concentrate. *Hydrometallurgy* 111:129–135
13. Cawthorn RG, Walraven F (1998) Emplacement and crystallization time for the Bushveld Complex. *J Petrol* 39:1669–1687
14. Kinloch ED (1982) Regional trends in the platinum-group mineralogy of the critical zone of the Bushveld Complex, South African Econ. Geology 77:1328–1347
15. Viljoen M (2016) (2016) The Bushveld complex-host to the world's largest platinum, chromium and vanadium resources. *Episodes* 39:238–268. <https://doi.org/10.18814/epiiugs/2016/v39i2/95777>
16. Shamaila S, O'Connor CT (2008) The role of synthetic minerals in determining the lative flotation behaviour of Platreef PGE tellurides and arsenides. *Miner Eng* 21:899–904
17. Vermaak MKG (2005) “Fundamentals of the flotation behaviour of palladium bismuth tellurides”, PhD thesis, University of Pretoria
18. Kinnaird JA (2005) The Bushveld large igneous province. Review Paper, The University of the Witwatersrand, Johannesburg, South Africa, pp. 1–39
19. Mwase JM, Petersen J, Eksteen JJ (2012) Assessing a two-stage heap leaching process for Platreef flotation concentrate. *Hydrometallurgy* 129–130:74–81. <https://doi.org/10.1016/j.hydromet.2012.09.007>
20. Corin KC, McFadzean BJ, Shackleton NJ et al (2021) Challenges related to the processing of fines in the recovery of platinum group minerals (PGMs). *Minerals* 11(533):1–17. <https://doi.org/10.3390/min11050533>
21. McLaren CH, De Villiers JP (1982) The platinum-group chemistry and mineralogy of the UG-2 chromitite layer of the Bushveld complex. *Econ Geol* 77(6):1348–1366
22. Mokadze AM, Ndlovu S, Shemi A et al (2021) The reduction of chrome in UG-2 flotation concentrate by hydrometallurgical means. *Int J Mineral Proc Extractive Metal* 6(3):41–52
23. Cawthorn RG (1999) Platinum-group element mineralization in the Bushveld Complex—a critical reassessment of geochemical models. *S Afr J Geol* 2(3):268–281.
24. Du Preez RC (2010) Effect of lime additions and bulk chromium content on chromium deportment in smelter matte-slag systems (M.Sc. Thesis, Stellenbosch: Stellenbosch University).
25. Eksteen JJ, Van Beek B, Bezuidenhout GA (2011) Cracking a hard nut: an overview of Lonmin's operations directed at smelting

- of UG2-rich concentrate blends. *J South Afr Inst Min Metall* 111(10):681–690
26. Ritchie S, Eksteen JJ (2011) Investigating the effect of slag bath conditions on the existence of “mushy” zones in PGM smelting furnaces using computational fluid dynamics. *Miner Eng* 24(7):661–675
 27. Eksteen JJ (2011) A mechanistic model to predict matte temperatures during the smelting of UG2-rich blends of Platinum Group Metal concentrate. *Miner Eng* 24(7):676–687
 28. Zheng WG, Din G et al (2019) Metals extraction from sulphide ores with microorganisms: the bioleaching technology and recent Developments. *Trans Indian Inst Met* 72(3):559–579
 29. Krebs W, Brombacher C, Bosshard PP (1997) Microbial recovery of metals from solids. *FEMS Microbiol Rev* 20:605–617
 30. Gadd GM (2000) Bio-remedial potential of microbial mechanisms of metal mobilization and immobilization. *Curr Opin Biotechnol* 11(3):271–279. [https://doi.org/10.1016/S0958-1669\(00\)00095-1](https://doi.org/10.1016/S0958-1669(00)00095-1)
 31. Ndlovu S (2008) Biohydrometallurgy for sustainable development in the African minerals industry. *Hydrometallurgy* 91(1–4):20–27
 32. Adams M, Liddell K, Holohan T (2011) Hydrometallurgical processing of Platreef flotation concentrate. *Miner Eng* 24:545–550
 33. Zhuang WQ, Fitts JP, Ajo-Frankline CM (2015) Recovery of critical metals using biometallurgy. *Curr Opin Biotechnol* 33(14):327–335
 34. Kumar A, Saini HS, Şengör S (2021) Bioleaching of metals from waste printed circuit boards using bacterial isolates native to abandoned gold mine. *Biomaterials* 34(5):1043–1058. <https://doi.org/10.1007/s10534-021-00326-9>
 35. Bosecker K (1997) Bioleaching: metal solubilization by microorganisms. *FEMS, Microbiology Review* 20:591–604
 36. Asghari I, Mousavi SM, Amiri F (2013) Bioleaching of spent refinery catalysts: a review. *J Ind Eng Chem* 19(4):1069–1081
 37. Xinhui D, Runhua C, Shengnan Z (2019) Bioleaching Characteristics of Heavy Metals from Polluted Soil with Indigenous *Aspergillus Niger* F2. *J Biobased Mater Bioenergy* 13(9):401–409
 38. Faramarzi MA, Mogharabi-Manzari M, Brandl H (2020) Bioleaching of metals from wastes and low-grade sources by HCN-forming microorganisms. *Hydrometallurgy* 191:105228
 39. Marsh RM, Norris PR (1983) Mineral sulphide oxidation by moderately thermophilic acidophilic bacteria. *Biotechnol Lett*. <https://doi.org/10.1007/BF00130837>
 40. Gericke M, Pinches A (1999) Bioleaching of copper sulphide concentrate using extreme thermophilic bacteria. *Miner Eng* 12:893–904. [https://doi.org/10.1016/S0892-6875\(99\)00076-X](https://doi.org/10.1016/S0892-6875(99)00076-X)
 41. Brierley JA (2008) A perspective on developments in biohydrometallurgy. *Hydrometallurgy* 94(1–4):2–7
 42. Wang Y, Zeng W, Qiu G, Chen X, Zhou H (2014) A moderately thermophilic mixed microbial culture for bioleaching of chalcopryrite concentrate at high pulp density. *Appl Environ Microbiol* 80:741–750. <https://doi.org/10.1128/AEM.02907-13>
 43. Kölbl D, Memic A, Schnideritsch H, Wohlmuth D, Klösch G, Albu M, Giester G, Bujdoš M, Milojevic T (2022) Thermoacidophilic bioleaching of industrial metallic steel waste product. *Front Microbiol* 13:864411
 44. Norris PR, Laigle L, Ogden TJ, Gould OJ (2017) Selection of thermophiles for base metal sulfide concentrate leaching. Part I: Effect of temperature on copper concentrate leaching and silver recovery. *Miner Eng* 106:7–12
 45. Beck JV (1967) The role of bacteria in copper mining operations. *Biotechnol Bioeng* 9(4):487–497
 46. Konishi Y, Nishimura H, Asai S (1998) Bioleaching of sphalerite by the acidophilic thermophile *Acidianus brierleyi*. *Hydrometallurgy* 47(2–3):339–352
 47. Saitoh N, Nomura T, Konishi Y (2017) Bioleaching of low-grade chalcopryrite ore by the thermophilic archaean *Acidianus brierleyi*. *Solid State Phenom* 262:237–241
 48. Huber G, Spinnler C, Gambacorta A, Stetter KO (1989) *Metallosphaera sedula* gen. and sp. nov. Represents a new genus of aerobic, metal-mobilizing, thermoacidophilic archaeobacteria. *Syst Appl Microbiol* 12:38–47. [https://doi.org/10.1016/S0723-2020\(89\)80038-4](https://doi.org/10.1016/S0723-2020(89)80038-4)
 49. Auernik KS, Kelly RM (2010) Physiological versatility of the extremely thermoacidophilic archaeon *Metallosphaera sedula* supported by transcriptomic analysis of heterotrophic, autotrophic, and mixotrophic growth. *Appl Environ Microbiol* 76:931–935. <https://doi.org/10.1128/AEM.01336-09>
 50. Ai C, Yan Z, Chai H, Gu T, Wang J, Chai L (2019) Increased chalcopryrite bioleaching capabilities of extremely thermoacidophilic *Metallosphaera sedula* inocula by mixotrophic propagation. *J Ind Microbiol Biotechnol* 46:1113–1127. <https://doi.org/10.1007/s10295-019-02193-3>
 51. Mukherjee A, Wheaton GH, Blum PH, Kelly RM (2012) Uranium extremophily is an adaptive, rather than intrinsic, feature for extremely thermoacidophilic *Metallosphaera species*. *Proc Natl Acad Sci* 109(41):16702–16707
 52. Milojevic T, Kölbl D, Ferrière L, Albu M, Kish A, Flemming RL (2019) Exploring the microbial biotransformation of extraterrestrial material on nanometer scale. *Sci Rep* 9:18028. <https://doi.org/10.1038/s41598-019-54482-7>
 53. Milojevic T, Albu M, Kölbl D, Kothleitner G, Bruner R, Morgan ML (2021) Chemolithotrophy on the Noachian Martian breccia NWA 7034 via experimental microbial biotransformation. *Commun Earth Environ* 2:39. <https://doi.org/10.1038/s43247-021-00105-x>
 54. Mwase JM, Petersen J, Eksteen JJ (2014) A novel sequential heap leach process for treating crushed Platreef ore. *Hydrometallurgy* 141:97–104
 55. Hedrich S, Kraemer D, Junge M et al (2020) Bioprocessing of oxidized platinum group element (PGE) ores as pre-treatment for efficient chemical extraction of PGE. *Hydrometallurgy* 196:105419
 56. Nunan TO, Viana IL, Peixoto GC et al (2017) Improvements in gold ore cyanidation by pre-oxidation with hydrogen peroxide. *Miner Eng* 108:67–70
 57. Haffty J, Riley LB, Goss WD (1977) *A Manual on Fire Assaying and Determining of the Noble Metals in Geological Materials*. Geological Survey Bulletin 1445, Washington D.C.
 58. EPA 3050B (1996) *Acid Digestion of Solid Samples for Metals Analysis*. Alpha Analytical, Inc. Quality Manual. Mansfield Facility, Metals Digestion Department. ID No.:2148, Revision 3, pp. 1–12
 59. Nakamura K, Miki H, Amano Y (1990) Cell growth and accumulation of *Thiobacillus thiooxidans* S3 in a pH-controlled thiosulfate medium. *J General Appl Microbiol* 36:369–376
 60. Kovaříková H, Janáková I, Čablík V, Vrlíková V (2019) Bacterial leaching of polymetallic ores from Zlatý Chlum locality. *J Pol Miner Eng Soc*. <https://doi.org/10.29227/IM-2019-01-27>
 61. Rendón-Castrillón L, Ramírez-Carmona M, Ocampo-López C, Gómez-Arroyave L (2023) Bioleaching techniques for sustainable recovery of metals from solid matrices. *Sustainability* 15:10222. <https://doi.org/10.3390/su151310222>
 62. Daniel C (1959) Use of half normal plots in interpreting factorial two level experiments. *Technometrics* 1(4):311–341
 63. Tripathy SK, Murthy YR (2012) Modeling and optimization of spiral concentrator for separation of ultrafine chromite. *Powder Technol* 221:387–394
 64. Montgomery DC (2005) *Design and analysis of experiments*. John Wiley and Sons, New Jersey
 65. Suslow TV (2004) *Oxidation-reduction potential for water disinfection monitoring, control, and documentation*. University of California. <http://anrcatalog.ucdavis.edu/pdf/8149.pdf>.
 66. Li E, Mira De Orduna R (2009) A rapid method for the determination of microbial biomass by dry weight using a moisture analyser

- with an infrared heating source and an analytical balance. Lett Appl Microbiol. <https://doi.org/10.1111/j.1472-765X.2009.02789.x>
67. Qiu Y, Mao Z, Sun K et al (2022) Understanding the entrainment behaviour of gangue minerals in flake graphite flotation. Minerals 12(9):1068. <https://doi.org/10.3390/min12091068>
 68. Box GEP, Hunter WG, Hunter JS (1978) Statistics for Experimenters: An Introduction to Design, Data Analysis and Model Building. John Wiley, New York
 69. Vera M, Schippers A, Sand W (2013) Progress in bioleaching: Fundamentals and mechanisms of bacterial metal sulphide oxidation-Part A. Appl Microbiol Biotechnol 97:7529–7541
 70. Ijadi BM, Mousavi SM, Shojaosadati SA (2014) Bioleaching of heavy metals from spent household batteries using *Acidithiobacillus ferrooxidans*: statistical evaluation and optimization. Sep Purif Technol 132:309–316
 71. Nemati M, Lowenadler J, Harrison STL (2000) Particle size effects in bioleaching of pyrite by acidophilic thermophile *Sulfolobus metallicus* (BC). Appl Microbiol Biotechnol 53:173–179
 72. Torma AE, Walden CC, Brannon RMR (1970) Microbiological leaching of a sulphide concentrate. Biotechnol Bioeng 12:501–517
 73. Torma AE, Walden CC, Duncan DW (1972) The effect of carbon dioxide and particle surface area on the microbiological leaching of a zinc sulphide concentrate. Biotechnol Bioeng 14:777–786
 74. Toma MK, Ruklisha MP, Vanags JJ (1991) Inhibition of microbial growth and metabolism by excess turbulence. Biotechnol Bioeng 38:552–556
 75. Howard D, Crundwell FK (1999) A kinetic study of the leaching of chalcopyrite with *Sulfolobus metallicus*. In: Amils R, Ballester A (eds) Biohydrometallurgy and the environment toward the 21st Century, Part A. Elsevier, Amsterdam, pp 209–217
 76. d'Hugues P, Morin D, Foucher S (2001) HIOX Project: a bioleaching process for the treatment of chalcopyrite concentrates using extreme thermophiles. In: Ciminelli VST, Garcia O (eds) Biohydrometallurgy: fundamentals, technology and sustainable development, Part A. Elsevier, Amsterdam, pp 75–83
 77. Sissing A, Harrison SLT (2003) Thermophilic mineral bioleaching: a compromise between maximizing mineral loading and maximizing microbial growth and activity. J S Afr Inst Mining Metall 103 (Part 2): 139–142
 78. Jiang M, Zhao Q, Liu C (2014) Sulfuric acid leaching of South African chromite. Part 2: optimization of leaching conditions. Int J Miner Process 130:102–107
 79. Jones RT, Geldenhuys IJ (2011) The pros and cons of reductive matte smelting for PGMs. Miner Eng 24(6):495–498
 80. Vardar E, Eric RH, Letowski FK (1994) Acid leaching of chromite. Miner Eng 7(5–6):605–617
 81. Zuliani L, Serpico A, De Simone M, Frison N, Fusco S (2021) Biorefinery gets hot: thermophilic enzymes and microorganisms for second-generation bioethanol production. Processes. <https://doi.org/10.3390/pr9091583>
 82. Liddell KS, Adams MD (2012) Kell hydrometallurgical process for extraction of platinum group metals and base metals from flotation concentrates. J South Afr Inst Min Metall 112:31–36
 83. Jackson E (1986) Hydrometallurgical extraction and reclamation. Halsted Press, New York
 84. Garrels RM, Christ CL (2007) Solutions, minerals, and equilibria. Harper and Row, Michigan
 85. Mamindy-Pajany Y, Hurel C, Marmier N (2009) Arsenic adsorption onto hematite and goethite. C R Chim 12(8):876–881
 86. Solís-Marcial OJ, Lapidus GT (2014) Study of the dissolution of chalcopyrite in sulfuric acid solutions containing alcohols and organic acids. Electrochim Acta 140:434–437
 87. Zhao Q, Liu C, Shi P (2014) Sulfuric acid leaching of South African chromite. Part 1: study on leaching behaviour. Int J Miner Process 130:95–101
 88. Geveci A, Topkaya Y, Ayhan E (2002) Sulfuric acid leaching of Turkish chromite concentrate. Miner Eng 15(11):885–888
 89. Vandeperre LJ, Liska M, Al-Tabbaa A (2008) Microstructures of reactive magnesia cement blends. Cement Concr Compos 30(8):706–714
 90. Dachs E, Metz P (1988) The mechanism of the reaction of tremolite: results of powder experiments. Contribution Mineral Petrol 100:542–551
 91. Britannica (2019) Muscovite". Encyclopedia Britannica, 7 Jan. 2019, <https://www.britannica.com/science/muscovite-mineral>. Accessed 8 Aug 2022
 92. Liddell KS (2015) Hydrometallurgical Treatment Process for Extraction of Metals from Concentrates. Patent: WO 2014/009928 Al. AU.
 93. Xiao Z, Laplante AR (2004) Characterizing and recovering the platinum group minerals—A review. Miner Eng 17:961–979

Publisher's Note Springer Nature remains neutral with regard to jurisdictional claims in published maps and institutional affiliations.

Authors and Affiliations

A. Shemi^{1,2} · L. Chipise^{1,2} · C. S. Yah^{2,4} · A. Kumar^{1,2} · S. Moodley^{1,2,3} · K. Rumbold³ · G. Simate¹ · S. Ndlovu^{1,2} 

✉ S. Ndlovu
sehliselo.ndlovu@wits.ac.za

¹ School of Chemical and Metallurgical Engineering, University of the Witwatersrand, Johannesburg, South Africa

² DSI/NRF SARChI: Hydrometallurgy and Sustainable Development, University of the Witwatersrand, Johannesburg, South Africa

³ Department of Industrial Microbiology and Biotechnology, School of Molecular and Cell Biology, University of the Witwatersrand, Johannesburg, South Africa

⁴ Department of Internal Medicine, School of Clinical Medicine (SOCM), Faculty of Health Sciences, University of the Witwatersrand, Johannesburg, South Africa